PHYSIOLOGY

Context-dependent impact of the dietary non-essential amino acid tyrosine on *Drosophila* physiology and longevity

Hina Kosakamoto[1], Chisako Sakuma[1], Rina Okada[1], Masayuki Miura[2], Fumiaki Obata[1,3]*

Dietary protein intake modulates growth, reproduction, and longevity by stimulating amino acid (AA)–sensing pathways. Essential AAs are often considered as limiting nutrients during protein scarcity, and the role of dietary non-essential AAs (NEAAs) is less explored. Although tyrosine has been reported to be crucial for sensing protein restriction in *Drosophila* larvae, its effect on adult physiology and longevity remains unclear. Here, using a synthetic diet, we perform a systematic investigation of the effect of single NEAA deprivation on nutrient-sensing pathways, reproductive ability, starvation resistance, feeding behavior, and life span in adult female flies. Specifically, dietary tyrosine deprivation decreases internal tyrosine levels and fecundity, influences AA-sensing machineries, and extends life span. These nutritional responses are not observed under higher total AA intake or in infertile female flies, suggesting a context-dependent influence of dietary tyrosine. Our findings highlight the unique role of tyrosine as a potentially limiting nutrient, underscoring its value for dietary interventions aimed at enhancing health span.

INTRODUCTION

Dietary restriction (DR) has been shown to extend life span in organisms ranging from yeast to primates, often at a reproduction cost (*1*–*6*). As a key macronutrient, protein is an important factor in determining the life span, growth, and reproduction of organisms. Since 1928, when McCay *et al.* (*7*) reported that trout fed a protein-restricted diet lived longer, the importance of dietary protein in life-span regulation has been controversial. Detailed nutritional analyses in *Drosophila melanogaster* have subsequently shown that the effect of DR on both life span and reproduction is not due to the limitation of calories but rather due to a decrease in protein intake (*8*, *9*). Life-span extension by protein restriction has also been reported in rodents and is frequently accompanied by metabolic and behavioral changes, such as improved glucose tolerance, insulin sensitivity, energy expenditure, and increased food intake (*10*–*12*).

Amino acids (AAs), the components of protein, were classified as essential AAs (EAAs) or non-essential AAs (NEAAs) nearly a century ago. Given the nature of NEAA biosynthesis in animals, EAAs are considered to play an important role as nutrient cues. For example, supplementing EAAs, but not NEAAs, under DR conditions has been shown to suppress life-span extension in *Drosophila*, supporting the idea that sensing EAAs is important for regulating life span (*13*). Some EAAs, such as methionine (Met), tryptophan, and branched chain AAs (BCAAs, leucine, isoleucine, and valine) are involved in longevity regulation (*14*–*24*). For example, Met restriction has been demonstrated to extend life span in organisms ranging from yeast to mice (*13*, *14*, *16*–*18*, *23*, *24*).

In flies, life-span extension due to Met restriction has been demonstrated only under conditions of limited (40%) total AA availability (*16*). In contrast, our previous study found that Met restriction extends life span even under conditions of 100% AA availability, provided that an exome-matched version of a synthetic diet (or so-called holidic medium) is used (*17*). Life-span extension is most pronounced when Met is restricted in early adulthood, with only mild effects observed in middle or later life stages (*17*). The effect of AA restrictions is highly contingent upon the animal model being used and the dietary context, even for EAAs. However, our understanding of the mechanisms by which each AA influences physiology and life span across various nutritional contexts remains incomplete. Compared to EAAs, the role of dietary NEAAs on animal physiology has been historically overlooked, given that they are not required for organismal growth, maintaining nitrogen balance, or maintaining internal levels of NEAAs regardless of dietary intake (*25*). However, we previously showed that some NEAAs are "nutritionally maintained" in *Drosophila* larvae, with their levels decreasing when dietary supply is insufficient (*26*). Such NEAAs include asparagine (Asn), serine (Ser), and tyrosine (Tyr) in *Drosophila*. The contribution of such NEAAs to organismal physiologies, however, has not been fully clarified so far.

AAs regulate nutrient-sensing mechanisms in animals, including insulin/insulin-like growth factor 1 signaling (IIS), mechanistic target of rapamycin complex 1 (mTORC1), and general control nonderepressible 2 (GCN2)–activating transcription factor 4 (ATF4) (*27*–*29*). mTORC1 is regulated by AAs both directly through AA sensor proteins and indirectly through IIS (*27*, *30*, *31*). AA deficiency activates the kinase GCN2, which senses uncharged tRNA or ribosomal stalling (*28*, *32*–*34*). These evolutionarily conserved signaling pathways act together to control metabolism, growth, reproduction, and longevity (*31*, *35*–*40*). For example, the genetic or pharmacological inhibition of IIS/mTORC1, or the activation of the GCN2-ATF4 pathway, improves metabolic homeostasis and extends life span, phenocopying dietary protein restriction (*35*–*39*). We previously found that the dietary deprivation of Tyr in particular elicits adaptive responses under conditions of protein restriction in *Drosophila* larvae through ATF4 activation, but independently of GCN2 (*26*). Larvae with Tyr deprivation exhibited suppressed protein translation and mTORC1 signaling in the fat body. Consequently, Tyr acts as a critical nutrient cue that signals protein scarcity, at least in *Drosophila* larvae.

[1]RIKEN Center for Biosystems Dynamics Research, Kobe, Hyogo 650-0047, Japan. [2]Department of Genetics, Graduate School of Pharmaceutical Sciences, The University of Tokyo, Bunkyo-ku, Tokyo 113-0033, Japan. [3]Laboratory of Molecular Cell Biology and Development, Graduate School of Biostudies, Kyoto University, Kyoto 606-8501, Japan.
*Corresponding author. Email: fumiaki.obata@riken.jp

Considering that Tyr is an important precursor for pigmentation and sclerotization during metamorphosis, the Tyr-sensing mechanism may be particularly relevant during the larval stage. Whether this mechanism is also conserved in adult flies has not been addressed.

At an organismal scale, AA levels are sensed systemically by sensory organs, the gastrointestinal tract, and internal organs, which provide integrated feedback to the central nervous system (*12*, *41*, *42*). These interorgan communication mechanisms control not only growth, reproduction, and life span but also appetite. In mice, ATF4 up-regulates the secretion of fibroblast growth factor 21 from the liver, which acts on the brain as a critical regulator of feeding behavior, as well as metabolic homeostasis and life span (*11*, *12*, *43*). Similarly, in *Drosophila*, AA restriction stimulates the secretion of a neuropeptide, CNMamide (CNMa), from the gut or the fat body, the counterpart of mammalian liver and white adipose tissue, via ATF4 and mTORC1 (*26*, *44*). CNMa binds to its receptor and enhances food intake or the preference for the L-form of EAAs (*26*, *44*). Protein feeding rapidly induces a neuropeptide hormone, *female-specific independent of transformer* (*fit*), which is regulated by the AA-sensing pathway, resulting in the suppression of protein appetite (*45*). Dietary AAs are also known to regulate other neuropeptides to control protein satiety (*46*, *47*). Thus, animals have mechanisms to sense AAs and modulate physiological and behavioral traits. However, the importance of NEAAs for such feeding regulation has not been fully investigated.

Here, using *D. melanogaster* and an optimized synthetic diet, we systematically evaluated the involvement of dietary NEAAs in regulating phenotypes associated with protein restriction. Our findings revealed that under conditions of low AA availability and high AA demand, Tyr in particular becomes limiting AA. Specifically, under such conditions, Tyr regulates nutrient-sensing pathways, fecundity, metabolism, feeding behavior, and life span.

RESULTS

Dietary deprivation of Tyr extends life span

To evaluate the impact of dietary NEAA deprivation on life span, we used a synthetic diet to completely deplete 1 out of 10 NEAAs and assessed the effects on the life spans of wild-type female *D. melanogaster* Canton-S (Fig. 1, A to J). For this analysis, we used an exome-matched holidic medium with the total AA content decreased to 40%. This approach was based on empirical evidence suggesting that a reduction in total AA enhances sensitivity to individual AA restriction (*16*, *17*). Met, an EAA, was included for comparison (Fig. 1K). As expected, we found that the complete depletion of many NEAAs did not strongly affect life span ($P > 0.001$), while that of Met strongly shortened life span (Fig. 1, A to K). While partial Met restriction can be beneficial, total depletion has a detrimental effect on the life span (*17*). Deprivation of the two NEAAs, Asn and cysteine, led to a shortened life span (Fig. 1, B and D). In contrast, Tyr deprivation led to life-span extension (Fig. 1J). This effect was also observed in an outbred strain of w^{Dah} female flies (Fig. 1L), confirming the robustness of the observed phenotype. The unique response of life-span extension by restricting Tyr, as opposed to other NEAAs, prompted us to investigate the underlying nutritional mechanisms of sensing this AA.

Tyr deprivation decreases ovary size and fecundity

Since AAs affect a life-span reproduction trade-off, life-span extension by DR is often associated with decreased fecundity (*48*). To evaluate the effect of NEAA deprivation on fecundity, we counted the number of eggs laid within 24 hours following 1 week of dietary manipulation. The result showed that both Asn and Tyr deprivation significantly decreased fecundity ($P < 0.001$; Fig. 1M). Notably, the effect of Tyr was more pronounced than that of Asn, but much less severe than the impact of Met depletion, suggesting that the Tyr behaves as a semi-essential AA in this context (Fig. 1M). Given that the deprivation of Asn or Met shortened life span, the observed decrease in reproductive capacity is not entirely correlated with life span. Consistent with the decrease in fecundity, ovary size was reduced following Tyr deprivation (Fig. 1, N and O).

Tyr deprivation enhances starvation resistance and yeast preference

Another typical phenotype associated with protein/AA restriction in flies is enhanced starvation resistance (*17*, *49*). We found that deprivation of Asn, aspartic acid (Asp), Ser, or Tyr significantly increased starvation resistance ($P < 0.01$; fig. S1, A to K). Glutamine and proline deprivation also slightly increased starvation resistance (fig. S1, E and H). While Met and Asn deprivation both increased starvation resistance, we observed a concurrent decrease in life span (Fig. 1, B and K, S1B, K). These results suggest that the regulatory mechanisms underlying starvation resistance and life span are different, and/or that the duration of AA deprivation (1-week versus lifelong) leads to distinct outcomes. Tyr was the only AA that enhanced both starvation resistance and life span when depleted. We confirmed that this enhancement of starvation resistance with Tyr deprivation was further validated in w^{Dah} female flies (fig. S1L).

As a part of adaptive responses, protein restriction up-regulates the feeding preference for protein (*50*). Focusing on Tyr, we found that female flies, upon Tyr deprivation, showed an increased food preference for yeast extract over sucrose (Fig. 1P). This indicates that Tyr deprivation modifies the mechanisms underlying food choice determination. Together, we found that Tyr deprivation not only decreases fecundity but also increases starvation resistance, protein preference, and life span. These effects mirror the phenotype associated with overall protein restriction, suggesting that Tyr plays a critical role in the dietary regulation of these physiological processes.

Tyr, Asn, and Ser are nutritionally maintained NEAAs in female flies

Next, we quantified whole-body NEAAs upon the NEAA deprivation. As expected, a majority of the NEAA deprivations did not affect the internal NEAA levels, suggesting the idea that internal NEAA levels are maintained without dietary input (Fig. 2, A to J). We found that deprivation of Asn, Ser, or Tyr led to decreased internal AA levels (Fig. 2, B, I, and J). These findings are consistent with the fact that Tyr, Asn, and Ser are nutritionally maintained NEAAs in the larval stage or in adult males (*26*). The levels of Tyr and Asn decreased to approximately 30 and 37%, respectively, while Ser decreased to approximately 75%. Asn, Ser, and Tyr consistently affected starvation resistance, although Asp only affected starvation resistance without a decrease in internal Asp levels. The similar reduction in the internal AA levels by Asn and Tyr is notable, given that these two NEAAs have opposite effects on life span (Fig. 1, B and J). Our detailed phenotypic analysis of NEAA deprivations suggests AA-specific sensing and nutritional signaling.

By analyzing other AA levels upon Tyr deprivation with 40%AA, we found that many AAs including arginine, lysine, Met, threonine,

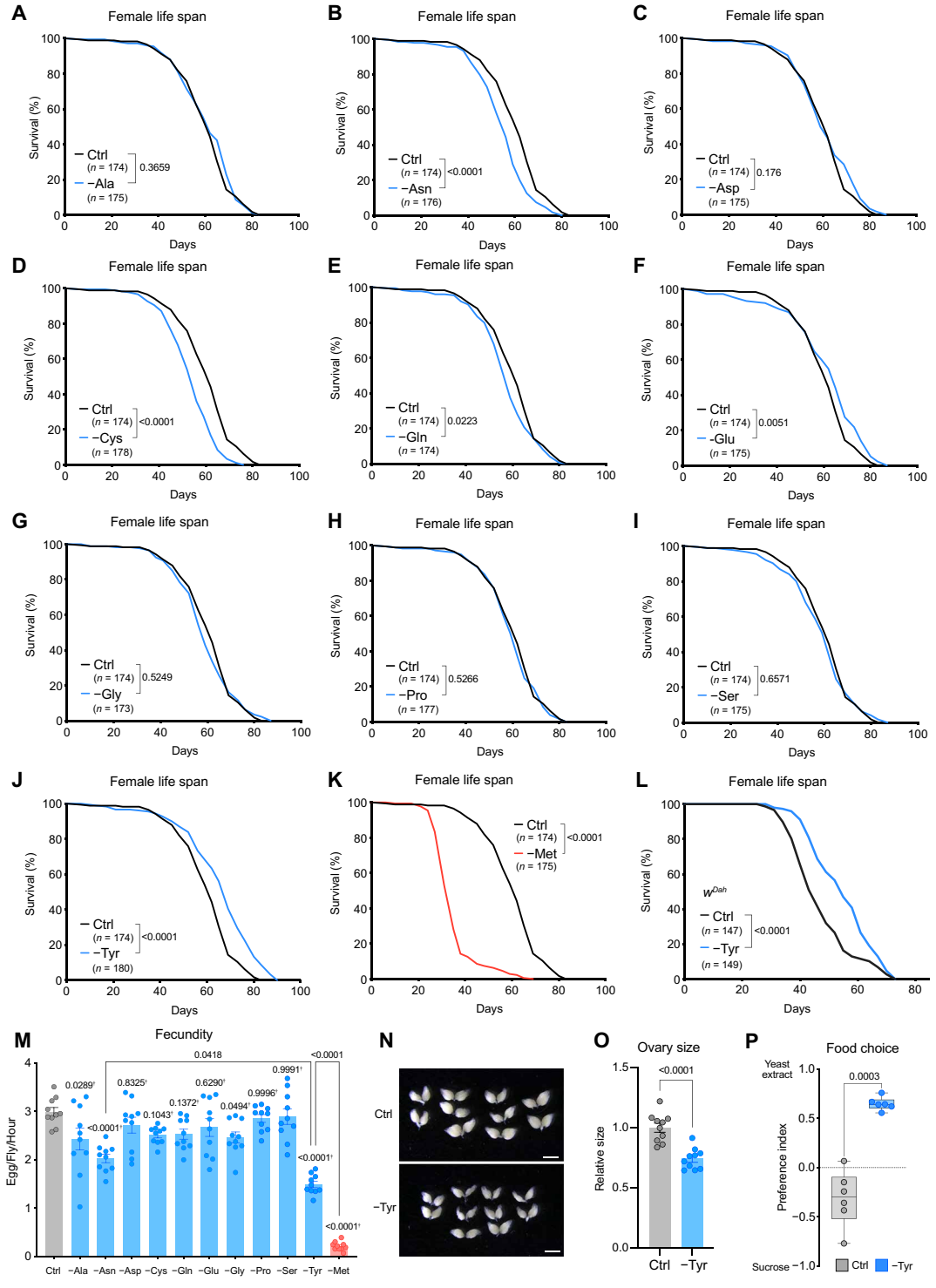

Fig. 1. Tyr deprivation extends life span, decreases fecundity, and increases yeast preference. (**A** to **K**) Life spans of female Canton-S flies with single NEAA deprivations (A to J) or Met deprivation (K). Sample sizes (*n*) are shown in the figure. (**L**) Life spans of female w^{Dah} flies with lifelong Tyr deprivation. Sample sizes (*n*) are shown in the figure. (**M**) Fecundity of Canton-S flies after single NEAA deprivations. $n = 10$. *P* values with a dagger (†) indicate the statistical comparisons with Ctrl. (**N** and **O**) Representative images of the ovaries with Tyr deprivation (N) and the quantification of ovary sizes (O). Scale bars, 1 mm. $n = 10$. (**P**) Food preference toward yeast extract compared to sucrose in female Canton-S flies after Tyr deprivation. $n = 6$. The graph shows the minimum, the lower quartile, the median, the upper quartile, and the maximum points. AA deprivations were performed through life (A to L), for 4 (M to O), or 7 days (P) from day 2. For the statistics, a log-rank test (A to L), one-way ANOVA with Holm-Šídák's multiple comparisons test (M), or a two-tailed Student's *t* test (O and P) was used. For all graphs other than (P), the means and SEM are shown. Data points indicate biological replicates.

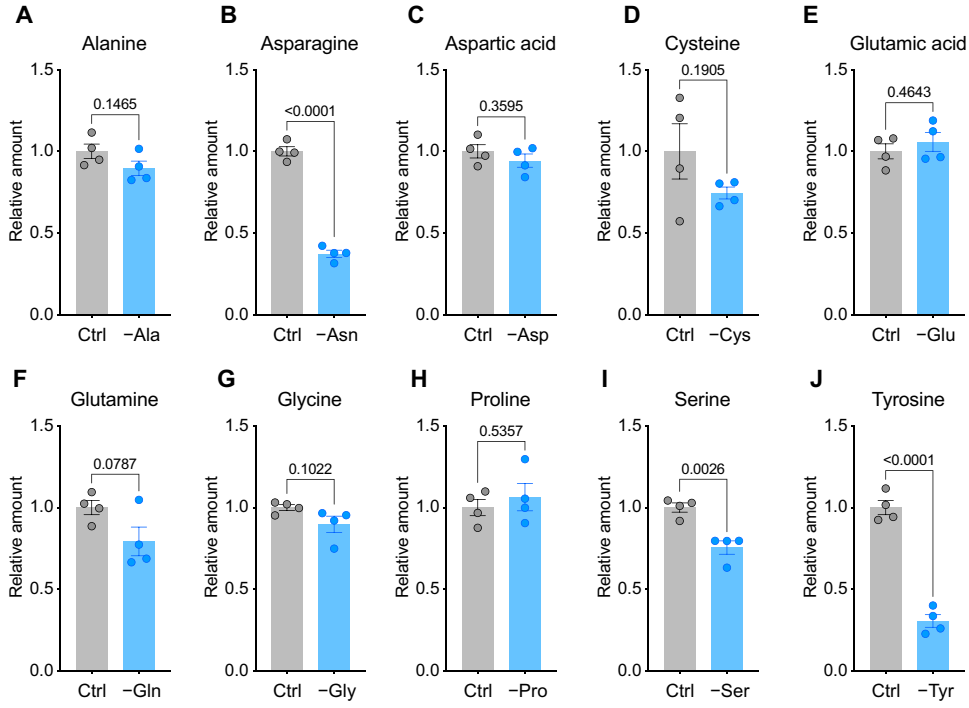

Fig. 2. Deprivations of Asn, Ser, and Tyr decrease their internal levels. (**A** to **J**) Quantification of internal NEAA levels in Canton-S female flies with single NEAA deprivations for 4 days from day 2. $n = 4$. For the statistics, a two-tailed Student's t test was used. For all graphs, the means and SEM are shown. Data points indicate biological replicates.

tryptophan, valine, Asn, and Ser were increased rather than decreased, while only glutamic acid was slightly decreased (fig. S2, A to R). The result suggests that sensing Tyr deficiency may alter metabolism, and perhaps intake or excretion of various AAs. It is also possible that free AAs are increased through enhanced protein degradation (e.g., autophagy).

Dietary Tyr is not critical when total AA intake is high

NEAAs are understood to be fully synthesized in the body. However, our analysis revealed that Tyr, among others, is nutritionally maintained and that its omission from the diet leads to protein restriction-like phenotypes. We wondered why the importance of dietary Tyr has not yet been appreciated. We investigated the effects of Tyr deprivation using higher dietary AA levels (i.e., 100% AA rather than 40% AA). Under conditions of increased total AA levels, Tyr deprivation did not affect life span, starvation resistance, or fecundity (Fig. 3, A to C). The basal level of internal Tyr remained unchanged between diets of 100 and 40% AA (Fig. 3D). Nonetheless, under conditions of reduced total AA, flies become more sensitized to Tyr deprivation (Fig. 3D), possibly due to a decrease in phenylalanine (Phe), the precursor of Tyr, in low AA conditions (Fig. 3E). Even under these conditions, Tyr deprivation did not further reduce Phe, suggesting that sensing Tyr scarcity does not enhance Tyr biosynthesis which consumes Phe. By adding back the Phe to Tyr-deprived diet, we observed the recovery of the fecundity (fig. S3A). Phe supplementation led to full recovery of internal Tyr level and canceled the Tyr deprivation effect on fecundity (fig. S3, A to C). The fecundity analysis also implies the irrelevance of Tyr metabolites on reproductive control (fig. S3A). Oviposition requires neuronal signaling involving octopamine secretion (*51*), but such a regulatory mechanism does not appear to play a role in the fecundity phenotype observed with Tyr deprivation (fig. S3A).

Tyr is not a limiting nutrient in males or sterile females

The dietary requirement of Tyr is affected not only by biosynthetic capacity but also by the consumption rate. Since egg laying is one of the most nutrient-demanding processes that female flies undertake, we used male flies as well as eggless female flies to test whether reproduction influences the Tyr deprivation phenotype. As expected, neither life-span extension nor increased starvation resistance was observed in Canton-S male flies (Fig. 3, F and G). Similarly, the loss of reproductive ability in ovo^{D1} female flies completely negated the life-span extension and starvation resistance phenotypes (Fig. 3, H and I). Furthermore, increased protein preference was observed in neither the male flies nor the infertile female flies (Fig. 3, J and K). We found that internal Tyr levels did not decrease following Tyr deprivation in infertile flies (Fig. 3L). This result suggests that the deprivation of the NEAA Tyr may become a limiting AA under conditions where they face a high demand for AAs and reduced total AA availability, highlighting a previously unidentified context-dependent response to AA restriction. As for male flies, it has been shown that Tyr deprivation in males decreases internal Tyr levels by approximately 36% (*26*). Therefore, it is unlikely that the absence of phenotypes in males is merely due to a lack of reduction in Tyr levels, as observed in infertile females. Although we cannot negate the possibility that the decrease in Tyr levels in males is not strong enough, we suspect that the phenotypic difference between the sexes may arise from as yet unknown causes.

Tyr regulates nutrient-sensing pathways

We then investigated the effects of dietary NEAAs on nutrient-sensing mechanisms. To assess ATF4 activity, we used a $4E\text{-}BP^{intron}$-*dsRed* reporter, in which the ATF4-binding sequence of an intron of

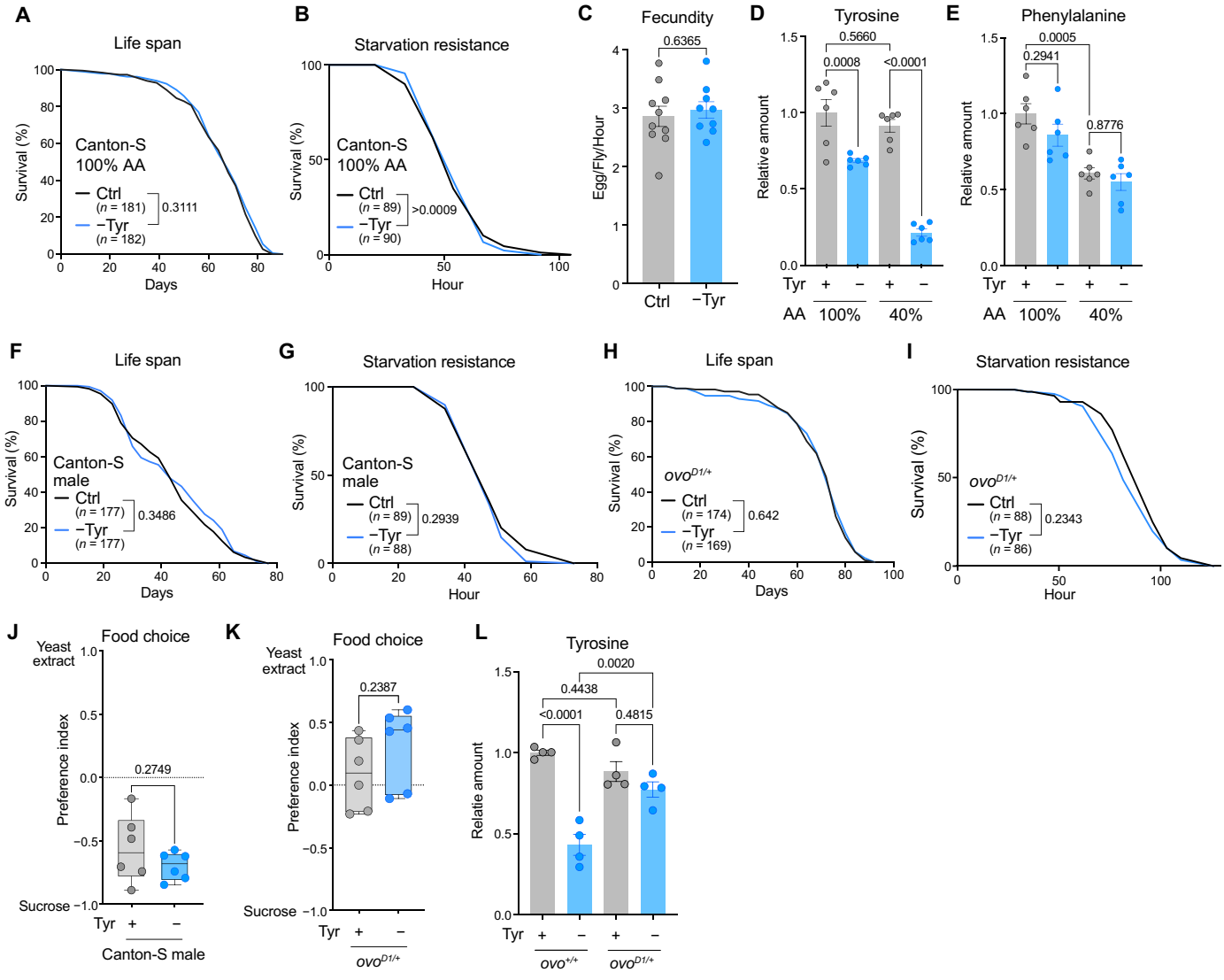

Fig. 3. Context-dependent impact of Tyr deprivation on physiology, behavior, and life span. (**A** and **B**) Life spans (A) and starvation resistance (B) of female Canton-S flies with Tyr deprivation from day 2 in the 100% AA condition. Sample sizes (*n*) are shown in the figure. (**C**) Fecundity of female Canton-S flies with Tyr deprivation in the 100% AA condition. $n = 10$. (**D** and **E**) Quantification of internal levels of Tyr (D) or Phe (E) in female Canton-S flies with Tyr deprivation in the 100 or 40% AA conditions. $n = 6$. (**F** to **I**) Life spans (F and H) and starvation resistance (G and I) of male Canton-S flies (F and G) or female $ovo^{D1/+}$ flies (H and I) with Tyr deprivation. Sample sizes (*n*) are shown in the figure. (**J** and **K**) Food preference toward yeast extract compared to sucrose in male Canton-S flies (J) or female $ovo^{D1/+}$ flies (K) after Tyr deprivation. $n = 6$. The graph shows the minimum, the lower quartile, the median, the upper quartile, and the maximum points. (**L**) Quantification of internal Tyr levels in female Canton-S flies ($ovo^{+/+}$) or $ovo^{D1/+}$ flies with Tyr deprivation. $n = 4$. Tyr deprivations were performed through life (A, F, and H), for 7 (B to E, G, and I to K), or 9 days (L) from day 2. For the statistics, a log-rank test (A, B, and F to I), a two-tailed Student's *t* test (C, J, and K), or one-way ANOVA with Holm-Šídák's multiple comparisons test (D, E, and L) was used. For all graphs except for (J) and (K), the means and SEM are shown. Data points indicate biological replicates.

eukaryotic initiation factor 4E-binding protein (*4E-BP*) is fused with the red fluorescent protein (RFP) dsRed (*26*, *52*). Among the NEAAs, only deprivation of Tyr significantly enhanced the reporter's fluorescence in the abdomen, suggesting an up-regulation of ATF4 activation in the adult fat body (Fig. 4, A and B). Even Met deprivation failed to increase the fluorescence of the ATF4 reporter, indicating that Tyr is a key regulator of ATF4. The adult fat body, which is also largely distributed in the head, showed pronounced enhancement of ATF4 reporter fluorescence with Tyr deprivation (Fig. 4, A and C). While Asn or Met deprivation also stimulated ATF4 activity in the head, the effect was considerably milder compared to Tyr deprivation (Fig. 4C). The careful observation revealed that the abdominal fat body attached to the abdominal carcass exhibited a marked increase in fluorescence following Tyr deprivation (Fig. 4D). The brain displayed neither basal nor increased ATF4 reporter fluorescence following Tyr deprivation (fig. S4A). Although baseline reporter fluorescence was observed in the gut and the Malpighian tubules of control flies, it was not enhanced by Tyr deprivation (fig. S4B). The ATF4 reporter activities remained unchanged in ovo^{D1} flies under Tyr deprivation, suggesting that the signaling activation is also dependent on reproductive activity (Fig. 4E).

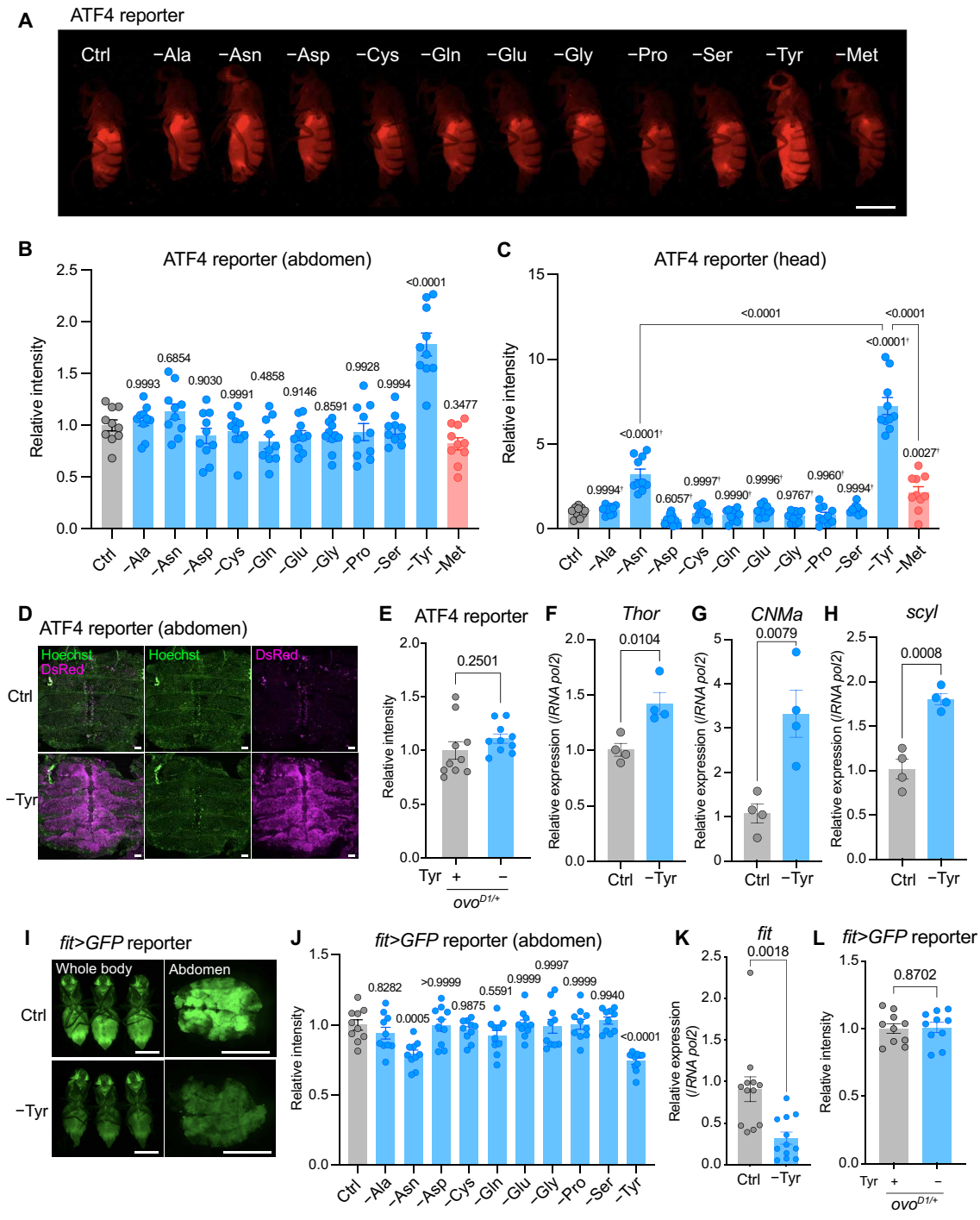

Fig. 4. Tyr deprivation stimulates nutrient-sensing pathways. (**A** to **C**) Representative images of ATF4 reporter *4E-BP*^{intron}*-dsRed* flies (A) and its quantifications of fluorescence in the abdomen (B) and in the head (C) with single NEAA or Met deprivations. The fluorescence between abdominal stripes on the dorsal side was quantified. $n = 10$. Scale bar, 1 mm. For (C), *P* values with a dagger (†) indicate the statistical comparisons with Ctrl. (**D**) Representative images of the dorsal side of the abdominal carcass of ATF4 reporter *4E-BP*^{intron}*-dsRed* flies with Tyr deprivation. Scale bars, 100 μm. (**E**) The quantification of the fluorescence in the abdomen of ATF4 reporter *4E-BP*^{intron}*-dsRed* flies with *ovo*$^{D1/+}$ transgene with Tyr deprivations. $n = 10$. (**F** to **H**) Quantitative reverse transcription polymerase chain reaction (RT-PCR) analysis of *Thor* (F), *CNMa* (G), and *scyl* (H) in the abdominal carcass of female Canton-S flies with Tyr deprivation. $n = 4$. (**I**) Representative images of whole bodies and the abdomens of *fit > GFP* reporter flies with Tyr deprivation. Scale bars, 1 mm. (**J**) The quantifications of fluorescence in the abdomen of *fit > GFP* reporter flies with single NEAA deprivations. $n = 10$. (**K**) Quantitative RT-PCR analysis of *fit* in the abdomen of female Canton-S flies with Tyr deprivation. $n = 12$. (**L**) The quantification of the fluorescence in the abdomen of *fit > GFP* flies with *ovo*$^{D1/+}$ transgene with Tyr deprivations. $n = 10$. AA deprivations were performed for 4 (A to E and L), 10 (F to H), or 7 days (I to K) from day 2. For the statistics, one-way ANOVA with Dunnett's multiple comparisons test (B and J), Holm-Šídák's multiple comparisons test (C), or a two-tailed Student's *t* test (E to H, K, and L) was used. For all graphs, the means and SEM are shown. Data points indicate biological replicates.

In the developing larva, yeast restriction or Tyr deprivation activates ATF4 and induces three target genes: *Thor* (an ortholog of mammalian *4E-BP*), *scylla* [*scyl*, an ortholog of mammalian *regulated in development and DNA damage responses 1* (*REDD1*) that suppresses mTORC1], and *CNMa* (*26*). Similarly, in adults, the expression of all three genes was induced by Tyr deprivation in the adult abdominal carcass (Fig. 4, F to H), confirming ATF4 activation in the adult fat body.

A neuropeptide hormone, FIT, has been reported to play a pivotal role in protein satiety (*45*). The expression of *fit* in the fat body is sensitive to dietary protein. Since Tyr deprivation increases the feeding preference for yeast (Fig. 1P), it appears that Tyr plays a role in the regulation of protein satiety. To investigate whether *fit* expression is regulated by Tyr or other NEAAs, we visualized its expression by using a *fit-Gal4*–driven green fluorescent protein (GFP). When *fit* > *GFP* expression was tested in the fat body, GFP fluorescence was suppressed following Tyr deprivation, especially in the abdomen (Fig. 4, I and J). We confirmed that *fit* expression of the abdominal carcass was suppressed by quantitative reverse transcription polymerase chain reaction (RT-PCR) (Fig. 4K). The *fit* > *GFP* reporter activities again remained unchanged in ovo^{D1} flies under Tyr deprivation (Fig. 4L). Our findings showed that only Tyr and Asn, the two nutritionally maintained NEAAs, affected the GFP expression (Figs. 4J and 2, B and J). These results suggest that Tyr, as well as Asn, to some extent, modulate nutrient-sensing pathways influenced by dietary protein.

To further clarify the effects of Tyr deprivation, we conducted RNA sequencing analysis on the abdominal carcass of female flies. The deprivation of Tyr resulted in the altered expression of 348 genes, with 149 being up-regulated and 199 down-regulated (data S1). Gene Ontology analysis revealed that up-regulated genes were associated with the forkhead box, sub-group O (FoxO) signaling pathway, autophagy, longevity-regulating pathway, and the mTOR signaling pathway, indicating a typical DR response (Fig. 5A). We found that the expression of *foxo* and its target genes, *Insulin-like receptor* (*InR*) and *Ecdysone-inducible gene L2* (*ImpL2*), was induced by Tyr deprivation (data S1). Other components of the insulin signaling pathway, including *Phosphoinositide-dependent kinase 1* (*Pdk1*) and *Akt kinase* (*Akt*), were also up-regulated (data S1), likely as a feedback mechanism to regulate the IIS pathway. Other up-regulated genes include *Autophagy-related 17* (*Atg17*), *Autophagy-related 101* (*Atg101*), *CREB-regulated transcription coactivator* (*Crtc*), and many mTORC1-related genes such as *Repressed by TOR* (*REPTOR*), *missing oocyte* (*mio*), and *Late endosomal/lysosomal adaptor, MAPK and MTOR activator 2* (*Lamtor2*). The induction of autophagy-related genes and mTORC1 suppressor *scyl* suggests the inactivation of mTORC1 signaling. We found that the Tyr deprivation suppressed the phosphorylation of ribosomal protein S6, indicating the down-regulation of mTORC1 activity (fig. S5, A and B). The induction of mTORC1 signaling components (*mio* and *Lamtor2*) might, therefore, reflect the feedback response of the suppressed mTORC1 activity, similar to the case of insulin signaling.

Tyr deprivation induces cuticle-related genes and suppresses immune responses

The other genes up-regulated by Tyr deprivation contained those predominantly expressed in the carcass or associated with chitin-binding (data S1), such as *neuropeptide-like precursor 3* (*Nplp3*), *CG11382* (an ortholog of *hornerin* in other *Drosophila* species), *CG7203* (an ortholog of *adult cuticle protein 1*), *CG30281* [an ortholog of *microfibril associated protein 4* (*MFAP4*)], *Chitin deacetylase-like 5* (*Cda5*), *Cuticular protein 49Ae* (*Cpr49Ae*), and *CG15784* (another ortholog of *hornerin*). Since the Tyr degradation pathway is regulated in the larval epidermis (*53*), Tyr might affect epidermal tissue in the adult abdomen. The expression of three genes encoding the Tyr catabolic enzymes *Tyrosine aminotransferase* (*Tat*), *4-hydroxyphenylpyruvate dioxygenase* (*Hpd*), and *Glutamate oxaloacetate transaminase 2* (*Got2*) was down-regulated upon Tyr deprivation (data S1). In the larval epidermis, IIS regulates *Hpd* suppression upon a low protein diet, and adenosine 5′-monophosphate–activated protein kinase (AMPK) regulates *Hpd* induction upon a high protein diet or a high Tyr diet (*53*). The phosphorylation of AMPK in adult abdominal carcass was not changed upon Tyr deprivation (fig. S5, C and D), suggesting that AMPK is not involved in the phenotypes of Tyr deprivation in adult flies.

Gene Ontology analysis of the down-regulated genes indicated that the Toll and Imd signaling pathways are inhibited upon Tyr deprivation (Fig. 5B). Numerous genes encoding antimicrobial peptides, the Turandot family of proteins, and peptidoglycan recognition proteins were down-regulated (data S1). Paradoxically, despite the suppression of these pathways, the immune response inducible nuclear factor κB *Relish* (*Rel*) itself was up-regulated by Tyr deprivation. A previous study showed that mTORC1 positively regulates Toll and Imd signaling via nuclear localization of Rel (*54*). Suppression of mTORC1 signaling might be the cause of immunosuppression by Tyr deprivation. However, the physiological relevance of the suppressed immune signaling is unclear since the basal expression is low (data S1). We also confirmed that the expression of the neuropeptide *fit* was suppressed by Tyr deprivation (data S1).

Nutrient-sensing pathways interact and affect physiologies upon Tyr deprivation

Since our RNA sequencing analysis and the fluorescent reporter analyses suggested the involvement of the AA-sensing mechanisms in Tyr sensing, we performed genetic experiments to clarify their epistatic relationships. First, we confirmed that knockdown or overexpression of *ATF4* suppressed or enhanced ATF4 reporter fluorescence, respectively (Fig. 5, C and D). In contrast, knockdown of *GCN2* did not suppress the reporter activity (Fig. 5C), suggesting that the activation of ATF4 by Tyr deprivation operates independently of GCN2, as is the case in the larval fat body (*26*). We also found that activation of mTORC1 via overexpression of *Ras homolog enriched in brain* (*Rheb*) did not affect ATF4 reporter fluorescence (Fig. 5D). The induction of the mTORC1 inhibitor *scyl* was suppressed by ATF4 knockdown (Fig. 5F). These findings suggested that ATF4 functions upstream of mTORC1, but not in the reverse direction.

Previously, mTORC1 has been implicated in the regulation of *fit*, as evidenced by the suppression of expression following rapamycin treatment (*45*). To clarify whether this mechanism also applies to our model of flies with Tyr deprivation, we attempted to restore the decrease in *fit* expression. Unexpectedly, *Rheb* overexpression failed to completely inhibit the diminished fluorescence of *fit* > *GFP* caused by Tyr deprivation (Fig. 5F). Knockdown of *Increased minichromosome loss 1* (*Iml1*), a component of GAP Activity Toward Rags1, which is supposed to increase mTORC1 activity, slightly increase the basal fluorescence of *fit* > *GFP* upon control diet, but it did not suppress the decline of GFP fluorescence upon Tyr deprivation at all (fig. S6A). This result suggested that the mTORC1 activity in the fat body did not regulate the suppression of *fit* during Tyr scarcity. Similarly, ATF4 did not appear to play a role in *fit* suppression (Fig. 5F).

A

GO term (up)	Count	%	*P* value
FoxO signaling pathway	7	4.73	0.00012
Autophagy	7	4.73	0.00304
Longevity regulating pathway	4	2.70	0.03011
mTOR signaling pathway	5	3.38	0.03446
Insect hormone biosynthesis	3	2.03	0.04365

B

GO term (down)	Count	%	*P* value
Toll and Imd signaling pathway	7	3.54	0.00254
Phenylalanine metabolism	3	1.52	0.00743
Sphingolipid metabolism	4	2.02	0.01491
Cysteine and methionine metabolism	4	2.02	0.02399
Folate biosynthesis	4	2.02	0.02944
Glycerolipid metabolism	4	2.02	0.03340

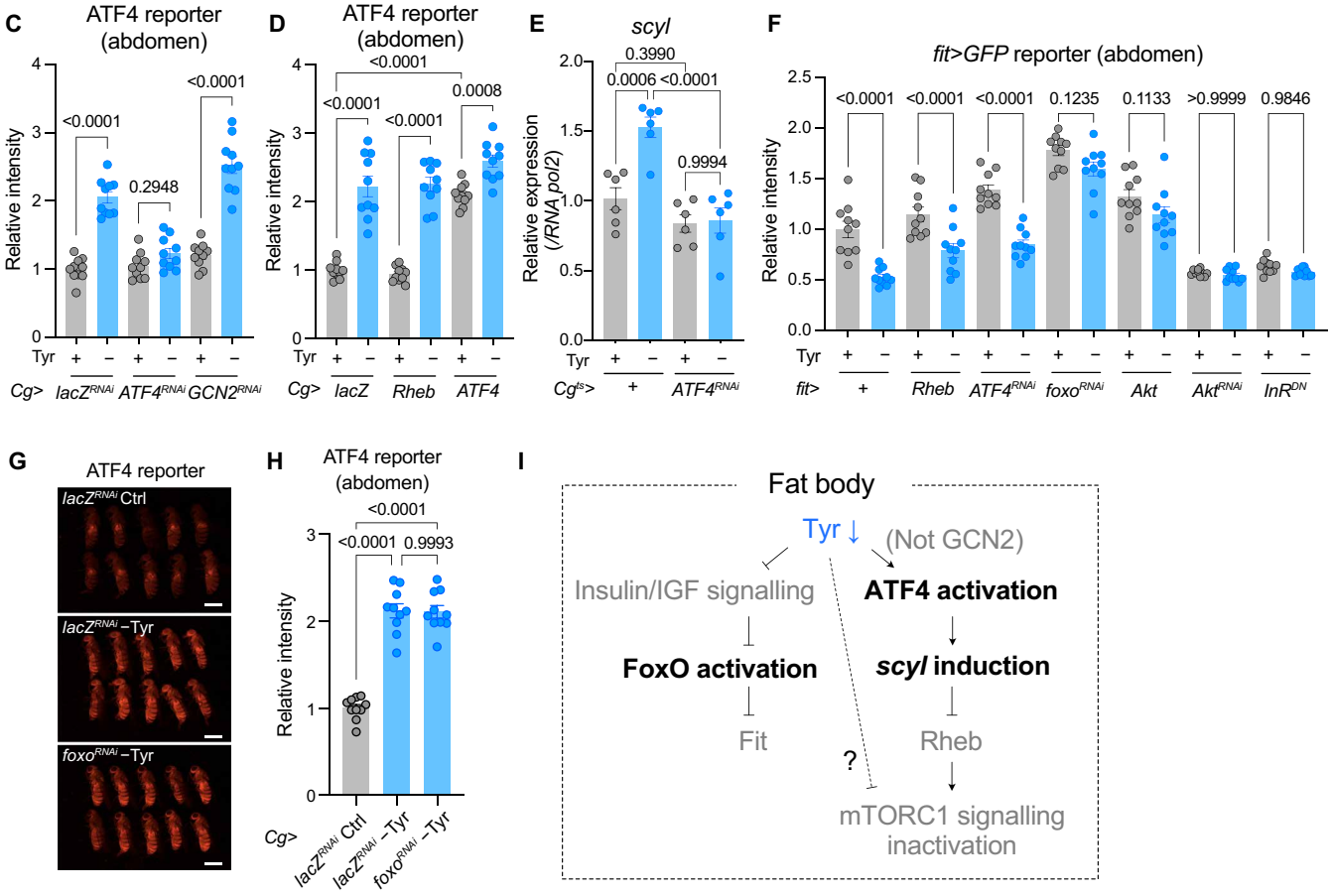

Fig. 5. Epistatic relationship of nutrient-sensing pathways involved in Tyr deprivation. (**A** and **B**) Gene Ontology analysis of up-regulated (A) and down-regulated (B) genes in the abdominal carcasses of female Canton-S flies with Tyr deprivations. (**C** and **D**) The quantifications of fluorescence in the abdomen of ATF4 reporter *4E-BP*^{intron}*-dsRed* flies with Tyr deprivations. The knockdown of *lacZ* (control), *ATF4*, and *GCN2* was conducted by using fat body driver *Cg-Gal4* (C). The overexpression of *lacZ* (control), *Rheb*, and *ATF4* was conducted by using fat body driver *Cg-Gal4* (D). $n = 10$. (**E**) Quantitative RT-PCR analysis of *scyl* in the abdominal carcasses of female flies with Tyr deprivation. The knockdown of *ATF4* was conducted by using fat body driver *Cg-Gal4* combined with *tub-Gal80*^{ts}. The flies were reared at 18°C until 4 days after eclosion and transferred to 29°C while Tyr was depleted. $n = 6$. (**F**) The quantifications of fluorescence in the abdomen of *fit > GFP* reporter flies with Tyr deprivation. Overexpression of *Rheb*, *Akt*, or *InR*^{DN} and knockdown of *ATF4*, *foxo*, or *Akt* were conducted using a *fit-Gal4* driver. Canton-S was crossed with *fit-Gal4* as a control. $n = 10$. (**G** and **H**) Representative images of ATF4 reporter *4E-BP*^{intron}*-dsRed* flies (G) and its quantifications of the fluorescence in the abdomen (H) with Tyr deprivations. $n = 10$. Scale bars, 1 mm. (**I**) The nutritional signaling pathways altered by Tyr deprivation in the fat body. AA deprivations were performed for 10 (A and B), 4 (C, D, G, and H), or 7 days (E and F) from day 2. For the statistics, one-way ANOVA with Holm-Šídák's multiple comparisons test was used (C to F and H). For all graphs, the means and SEM are shown. Data points indicate biological replicates.

Based on transcriptome data, we next explored the involvement of the IIS/FoxO pathway in *fit* regulation. Knockdown of *foxo* or overexpression of *Akt* increased the basal fluorescence of *fit > GFP* and completely blocked its decrease under Tyr deprivation (Fig. 5F). In addition, knockdown of *Akt* or overexpression of the dominant-negative form of *InR* decreased the basal fluorescence of *fit > GFP*, regardless of dietary Tyr (Fig. 5F). These results strongly suggest that *fit* suppression is a consequence of decreased IIS and increased FoxO activity resulting from Tyr deprivation.

The ATF4 reporter fluorescence was not suppressed by *foxo* knockdown, suggesting that the FoxO does not activate ATF4 (Fig. 5, G and H). Together, our findings show that Tyr deprivation activates ATF4 by an unknown mechanism that is independent of *GCN2*, *Rheb*, and *foxo*. The activation of ATF4 may lead to the

suppression of mTORC1 signaling via the induction *scyl*. Concurrently, Tyr deprivation diminishes IIS signaling and activates FoxO, which, in turn, suppresses the expression of the protein satiety hormone *fit* (Fig. 5I). We found that D-Tyr or L-DOPA can act as a substitute L-Tyr for the induction of *fit* (fig. S6B), suggesting that at least a part of the Tyr-sensing mechanism might involve a mechanism that detects the structural similarity, possibly the phenolic group, of Tyr. This finding contrasts with the unchanged fecundity phenotype observed with these compounds (fig. S3A), indicating that fecundity and nutrient-sensing mechanisms are not necessarily interconnected.

To test whether nutrient-sensing mechanisms are essential for the phenotypic outcomes of Tyr deprivation, we manipulated *ATF4*, *Rheb*, and *foxo* expression in the fat body and assessed the effect on starvation resistance and life span (fig. S7, A to F). We found that neither *ATF4* knockdown nor *Rheb* overexpression negated the increases in life span and starvation resistance (fig. S7, A, C, D, and F). Knockdown of *Iml1* did not abolish the increased starvation resistance by Tyr deprivation, either (fig. S7G). In contrast, the knockdown of *foxo* in the adult fat body suppressed the life-span extension and mitigated the increase of starvation resistance by Tyr deprivation (fig. S7, B and E). The knockdown of *foxo* using whole-body driver *da-Gal4* completely suppressed the enhancement of starvation resistance, while the effect of *ATF4* knockdown was limited (fig. S7H). Thus, among multiple nutrient-responsive signaling pathways, FoxO signaling within the fat body mainly contributes to phenotypic changes induced by Tyr deprivation.

DISCUSSION

In this study, we described the physiological and molecular responses of adult female flies subjected to deprivations in single NEAAs. We found that three NEAAs, Asn, Ser, and Tyr, require dietary supplementation to maintain their internal levels, thus categorizing them as nutritionally maintained AAs. These findings corroborate the results obtained in our previous study in *Drosophila* larvae (*26*). Among these NEAAs, only Tyr deprivation elicits a typical DR response in female flies, i.e., decreased fecundity, increased starvation resistance, and extended life span. Dietary Tyr influences internal Tyr levels, ATF4 activity, and *fit* expression. While Asn deprivation affects fecundity and nutrient-sensing pathways similarly, it shortens rather than extends life span. We speculate that a specific adaptive response may be triggered only when Tyr is depleted, or that Asn deprivation incurs additional negative effects, which warrants further investigation. Since the classification of AAs has been historically based on essentiality for growth and fecundity, the importance of dietary NEAAs has been somewhat overlooked (*55*). A previous report showed that EAA/NEAA ratios affect mouse life span, suggesting that a high EAA/low NEAA diet can extend life span (*56*). While the focus on NEAA effects has been limited, we must consider the ratio of individual EAAs and NEAAs relative to total AA intake. The ingestion of NEAAs has been reported to suppress feeding behavior while increasing exploration in mice (*57*). This behavioral change is mediated by hypothalamic orexin/hypocretin neurons, which are activated by NEAAs but not EAAs (*57*, *58*). It has also been shown that ingestion of NEAAs, rather than EAAs, can increase pancreatic growth and protease production in rats (*59*). These results suggest that the contribution of dietary NEAAs can, in some cases, surpass that of dietary EAAs. Considering the accumulating evidence of NEAA function in various physiologies, the importance of NEAAs should be reevaluated (*55*). Nevertheless, the negative impacts of NEAA deprivation on fecundity and life span are almost negligible or much less than those of EAAs. Focusing on dietary intake and metabolism of NEAAs offers a potentially promising avenue to delay aging, extend life span, and modulate feeding behavior with minimal negative effects on organismal growth and reproduction.

Although D-Tyr or L-DOPA cannot ameliorate the reduction in fecundity caused by Tyr deprivation, they restored decreased *fit* expression. This result implies that Tyr can function both as a building block and a signaling molecule that activates nutrient-sensing pathways. Although the precise mechanism underlying Tyr sensing remains to be elucidated, structural recognition of Tyr might be important for the stimulation. The neuropeptide FIT, which has been identified as the protein satiety hormone, is predominantly expressed in female flies (*45*). Our findings showed that the regulation of *fit* expression is dependent on the IIS/FoxO pathway. The transcriptome analysis consistently showed the induction of *foxo* and its target genes upon Tyr deprivation. It has been shown that FIT stimulates insulin-producing cells in the brain, changing their activity (*45*). The suppression of FIT can act as a feed-forward mechanism to inhibit IIS by interorgan communication, although the contribution of this neuropeptide to IIS activity and physiological traits, including life-span regulation, requires further clarification.

Tyr acts as a precursor of melanin, which plays a role in the encapsulation of pathogens (*60*). The process of melanization is also a characteristic phenomenon that occurs in the cuticles of adults. The up-regulation of several genes associated with cuticle function in the transcriptome analysis may represent an adaptive response to the scarcity of Tyr or its metabolites. It has been shown that the homeostasis of adult epidermal tissue declines during aging (*61*). While the contribution of cuticle function to life-span regulation is not well understood, the integrity of the cuticle as the outermost barrier could be important for maintaining organismal health.

Supplementation of the diet with Tyr has been demonstrated to prolong the life span of *Drosophila* (*62*). Given that Tyr is a precursor for neurotransmitters such as dopamine, restoring the decreased dopamine levels during aging might be crucial for extending the life span (*62*). Although our present study did not directly investigate the effect of Tyr deprivation on dopamine levels, inactivation of IIS and mTORC1 signaling in peripheral tissues by Tyr deprivation could potentially suppress organismal aging, thereby eventually counteracting the decrease in age-related dopamine loss. High Tyr intake can be beneficial for healthy individuals, but when degradation pathways are suppressed, Tyr can become cytotoxic due to its low solubility (*53*, *63*–*65*). Several reports have shown that high Tyr levels in circulation increase the risk of diabetes and obesity (*66*–*69*). Consequently, it is important to test the effects of high or low Tyr levels on the promotion of health span in different contexts. This nuanced effect is similar to that reported for the effects of BCAAs (*21*, *70*). While some studies have suggested that the restriction of BCAAs can extend life span (*14*, *21*, *22*), other studies have shown that supplementation with BCAAs can extend life span (*71*, *72*). Therefore, careful and quantitative analysis of AA restriction or AA supplementation on health and diseases in various contexts is necessary for developing dietary interventions to improve animal and human health span.

MATERIALS AND METHODS

Drosophila stocks and husbandry

Flies were reared on a standard yeast-based diet containing 4.5% cornmeal (Nippn Corporation), 6% brewer's yeast (HB-P02, Asahi Breweries), 6% glucose (Nihon Shokuhin Kako), and 0.8% agar (S-6, Ina Food Industries) with 0.4% propionic acid (FUJIFILM Wako Pure Chemical Corporation, 163-04726) and 0.15% butyl *p*-hydroxybenzoate (FUJIFILM Wako Pure Chemical Corporation, 028-03685). Flies were maintained at 25°C. To ensure synchronized development and constant density, embryos were collected using agar plates (2.3% agar, 1% sucrose, and 0.35% acetic acid) with a live yeast paste.

The fly lines used in this study were Canton-S, w^{Dah} (*13*), *4E-BP*^{intron}-*dsRed* (*52*), *fit-Gal4* (*45*), *Cg-Gal4* [Bloomington Drosophila Stock Center (BDSC), 7011], *da-Gal4* (*26*), *UAS-2×EGFP* (BDSC, 6874), *UAS-lacZ-RNAi* (from Richard Carthew, backcrossed eight times with $w^{Canton\text{-}S}$), *UAS-ATF4-RNAi* [Vienna Drosophila Resource Center (VDRC), 109014, backcrossed eight times with $w^{Canton\text{-}S}$], *UAS-foxo-RNAi* (BDSC, 32429), *UAS-Akt-RNAi* (BDSC, 33615), *UAS-ATF4* (FlyORF, F000106), *UAS-Rheb* (BDSC, 9689, backcrossed eight times with $w^{Canton\text{-}S}$), *UAS-Akt* (BDSC, 8191), *UAS-InR*^{DN} (BDSC, 8253), *UAS-Iml1-RNAi* (BDSC, 57492), *UAS-Iml1-RNAi* (VDRC, 110386), *tub-Gal80*^{ts} (BDSC, 7017), and *ovo*^{D1} (BDSC, 1309).

Dietary manipulations

The ingredients of the holidic medium used in our study were previously published (*17*). Unless noted, the total amount of AAs was adjusted to 40% of that found in the original exome-matched diet (*73*).

Life-span analysis

Adult flies were allowed to mate for 2 days after eclosion in a bottle. Subsequently, 30 female or male flies were allocated to vials containing holidic medium. Six vials containing 30 flies each were prepared for each condition. The flies were maintained at 25°C under 60% humidity and a 12-hour light:12-hour dark cycle. Flies were transferred to fresh vials every 3 to 4 days, and the number of dead or censored flies was counted.

Starvation resistance assay

Similar to the procedure for life-span analysis, adult flies were placed in vials with a specific diet 2 days after eclosion. Three vials containing 30 flies each were prepared for each condition. After 1 week, flies were transferred to vials containing 1% agar, and the number of dead flies was counted.

Fecundity analysis

Similar to the procedure for life-span analysis, at 2 days after eclosion, 17 female flies and 17 male flies were placed in vials containing a specific diet. Two vials containing a total of 34 flies per vial were prepared for each condition. After 1 week, flies were anesthetized quickly with CO_2 and reallocated to 10 vials containing each diet with three females and three males per vial. After 24 hours, the number of eggs laid on the medium was manually counted.

Imaging analysis

To analyze ovary size, dissected ovaries were placed in phosphate-buffered saline (PBS) on a silicone pad. Images were captured using a fluorescence stereomicroscope (Leica Microsystems GmbH, MZ10F). The area of the ovary from the top view was measured using the Fiji software (*74*). For whole-body reporter fluorescence, flies were immobilized on a CO_2 pad, and the RFP or GFP fluorescence images were captured using a fluorescence stereomicroscope (Leica Microsystems GmbH, MZ10F). To analyze ATF4 reporter fluorescence in the abdomen, flies were imaged from the lateral side to minimize the interference of the basal fluorescence in the gut and Malpighian tubules. A region between stripes of the dorsal abdomen was selected as a region of interest (ROI), and the fluorescence was quantified using Fiji software (*74*). To analyze the ATF4 reporter fluorescence in the head, the region adjacent to the eyes was selected as the ROI, and the fluorescence was quantified using Fiji software (*74*). The expression level of the *fit > GFP* reporter was quantified by measuring the fluorescence of the entire abdomen, delineated by elliptical selections using the Fiji software package (*74*).

For a more detailed analysis of reporter expression, tissues from adult flies were dissected in PBS and fixed with 4% paraformaldehyde in PBS. After fixation for 20 min at room temperature (RT), the sample was washed multiple times with PBST buffer (0.1% Triton X-100 with PBS) and incubated for at least 2 hours at RT in Hoechst 33342 (diluted to 0.4 mM; Invitrogen, H3570) at 1:100. After washing, tissues were mounted in 80% glycerol and observed under a confocal microscope (Leica Microsystems GmbH, TCS SP8).

Measurement of metabolites

Metabolites were measured by ultraperformance liquid chromatography–tandem mass spectrometry (LCMS-8050/LCMS-8060NX, Shimadzu Corporation) following the protocol outlined in the Primary metabolites package ver. 2 (Shimadzu Corporation) (*26*, *75*). Four whole bodies of female flies were homogenized in 160 μl of 80% methanol containing 10 μM internal standards (Met sulfone and 2-morpholinoethanesulfonic acid). After centrifugation at 15,000*g* and 4°C for 5 min, 150 μl of supernatant was mixed with 75 μl of acetonitrile and deproteinised. After centrifugation at 20,000*g* and 4°C for 5 min, the supernatant was applied to a prewashed 10-kDa centrifugal filter device (Pall Corporation, OD010C35). The flow-through from this step was completely evaporated using a centrifugal concentrator (TOMY SEIKO Co. Ltd., CC-105). The dried samples were reconstituted in ultrapure water and injected into the LC-MS/MS with a pentafluorophenylpropyl column [Discovery HS F5 (2.1 mm by 150 mm, 3 μm), Sigma-Aldrich Co. LLC] maintained at 40°C in the column oven. A gradient transition from solvent A (0.1% formic acid and water) to solvent B (0.1% formic acid and acetonitrile) for 20 min was used to separate solutes. The multiple reaction monitoring parameters were optimized by the injection of the standard solution, with peak integration and parameter optimization performed using LabSolutions software (Shimadzu Corporation). The mass spectrometry raw data generated in this study have been deposited in the DNA Data Bank of Japan (DDBJ) MetaboBank under accession codes MTBKS238, MTBKS239, MTBKS240, and MTBKS241 (https://ddbj.nig.ac.jp/public/metabobank/study/). The mass spectrometry data generated in this study are provided in data S2.

Feeding assay

A two-choice test on a petri dish was adapted from a previously established protocol (*76*). Adult flies were placed in vials containing a specific diet at 2 days after eclosion. Six vials containing 30 flies each were prepared for each condition. After 1 week, flies were transferred to vials containing 1% agar. To prepare the assay plate, four 2 cm–by–2 cm filter papers (No. 50, Advantec CO. LTD.) were placed separately on the 100-mm petri dishes. Two of the papers were soaked

with 150 μl of Milli-Q water. The remaining two papers were treated differently: one was soaked with a 150-μl solution of a 1% yeast extract and brilliant blue (0.125 mg/ml; FUJIFILM Wako Pure Chemical Corporation, 027-12842) and the other was soaked with a 150-μl solution of 5 mM sucrose and acid red 52 (0.25 mg/ml; FUJIFILM Wako Pure Chemical Corporation, 018-10012). After starvation for 24 hours, the flies were briefly anesthetized by cooling to 4°C for 10 min and then transferred to the assay plate. The plate was covered with aluminum foil and placed in an incubator at 25°C at 60% humidity for 2 hours. Subsequently, the plate was collected and placed in a freezer at −30°C for at least 2 hours. The color of the abdomen was classified as blue, purple, or red. The preference index (PI) for yeast was calculated as follows: PI [blue] = {*N* (blue) − *N* (red)}/{*N* (blue) + *N* (purple) + *N* (red)}. Vials with more than 30% colorless flies were excluded from the analysis.

RNA sequencing analysis and quantitative RT-PCR analysis

For RNA sequencing analysis, we dissected abdominal carcasses containing abundant fat bodies from 10 female individuals. Gut, Malpighian tubules, and ovaries were carefully removed from the abdomen to prevent contamination. Total RNA was purified from the samples using a ReliaPrep RNA Tissue Miniprep kit (Promega Corporation, z6112). Four samples were prepared for each experimental group. Library preparation was performed by the RIKEN BDR Technical Support Facility using an Illumina Stranded mRNA Prep Ligation kit (96 samples) (Illumina K.K., 20040534) and IDT for Illumina RNA UD Indexes Set A Ligation kit (Illumina K.K., 20040553). The optimal number of PCR cycles was determined by real-time PCR using KAPA SYBR FAST qPCR Master Mix (F. Hoffmann-La Roche Ltd., KK4603). The library quality was verified using the TapeStation HS D1000 assay. The library samples were forwarded to AZENTA for RNA sequencing using an Illumina HiSeq X (Illumina K.K.). The paired-end 150–base pair sequence data were analyzed as follows: A quality check of the raw reads was performed by FastQC (v0.12.1) (*77*) and MultiQC (v1.14) (*78*). The raw reads were then filtered to remove the adaptors and low-quality bases using Trim Galore (v0.6.10) (*79*). Filtered reads were aligned to the *Drosophila* genome (BDGP6.46) using Hisat2 (v2.2.1) (*80*). The read counts were calculated using StringTie (v2.2.1) (*81*). Differentially expressed genes were identified using edgeR (v4.0.6) (*82*). RNA sequencing data have been deposited at the DDBJ under accession number PRJDB17577.

For quantitative RT-PCR analysis, total RNA was purified from the abdominal carcasses of five adult female flies, as described above, using a ReliaPrep RNA Tissue Miniprep kit (Promega Corporation, z6112). The cDNA was synthesized from 400 ng of deoxyribonuclease-treated total RNA using the ReverTra Ace Master Mix (Toyobo Co. Ltd., FSQ-201). Quantitative RT-PCR was performed using Taq Pro Universal SYBR qPCR Master Mix (Vazyme Biotech Co. Ltd., Q712-02-AA) and qTOWER^3 G (Analytik Jena GmbH+Co. KG) using *RNA pol2* as an internal control. Primer sequences are listed in table S1.

Western blot analysis

The abdominal carcass from eight female flies was dissected in PBS and homogenized in 50 μl of radioimmunoprecipitation assay buffer (FUJIFILM Wako, 188-02453) supplemented with protease inhibitor (FUJIFILM Wako, 165-26021) and phosphatase inhibitor cocktails (Roche, 4906845001). The supernatant was collected after centrifugation, and the protein amount was quantified by BCA assay (FUJIFILM Wako, 164-25935). The samples were mixed with 6× SDS–polyacrylamide gel electrophoresis (SDS-PAGE) sample buffer (Nacalai, 09499-14), and 10-μg proteins were subjected to standard SDS-PAGE. Gels were transferred to the polyvinylidene difluoride membrane and blocked by EveryBlot blocking buffer (Bio-Rad, 12010020). Primary antibodies used in the study were anti–α/β-tubulin (1:1000 dilution; Abcam, ab44928), anti-histone H3 (1:1000 dilution; CST, 1B1B2), anti–phospho-S6 [1:2000 dilution (*26*)], anti–phospho-AMPKα (1:500 dilution; CST, 2535S), and anti–total AMPKα (1:200 dilution; CST, 2532S). Horseradish peroxidase (HRP)–conjugated secondary antibodies were anti-mouse immunoglobulin G (IgG), HRP-linked antibody (1:1000 dilution; CST, 7076S) and anti-rabbit IgG, HRP-linked antibody (1:1000 dilution; CST, 7074S). The signals were visualized by chemiluminescence using Immobilon (Millipore, WBLUF0100) and detected by Amersham ImageQuant 800 (Cytiva).

Statistical analysis

Statistical analysis was performed using GraphPad Prism 10 (MDF Co. Ltd.). The sample size was determined empirically. To eliminate biological bias, the flies were randomly distributed onto each diet. All data points were biological, not technical, replicates. No data were excluded. Since the experiment planner (H.K.) and the experimenter were the same person, most experiments were not conducted in a blinded manner. For the experiments on life span with deprivations of specific NEAAs, a different person (R.O.) conducted the experiments without prior bias. An unpaired and two-sided Student's *t* test was used to compare samples. One-way analysis of variance (ANOVA) with Holm-Šídák's multiple comparisons test was used to compare groups. One-way ANOVA with Dunnett's multiple comparisons test was used to compare against a control sample. All experimental results were repeated at least twice to confirm reproducibility. Bar graphs are drawn as the means and SEM.

Supplementary Materials

The PDF file includes:
Figs. S1 to S7
Table S1
Legends for data S1 and S2

Other Supplementary Material for this manuscript includes the following:
Data S1 and S2

REFERENCES AND NOTES

1. L. Fontana, L. Partridge, V. D. Longo, Extending healthy life span—From yeast to humans. *Science* **328**, 321–326 (2010).
2. L. Fontana, L. Partridge, Promoting health and longevity through diet: From model organisms to humans. *Cell* **161**, 106–118 (2015).
3. P. Kapahi, M. Kaeberlein, M. Hansen, Dietary restriction and lifespan: Lessons from invertebrate models. *Ageing Res. Rev.* **39**, 3–14 (2017).
4. N. M. Templeman, C. T. Murphy, Regulation of reproduction and longevity by nutrient-sensing pathways. *J. Cell Biol.* **217**, 93–106 (2018).
5. C. L. Green, D. W. Lamming, L. Fontana, Molecular mechanisms of dietary restriction promoting health and longevity. *Nat. Rev. Mol. Cell Biol.* **23**, 56–73 (2022).
6. V. D. Longo, R. M. Anderson, Nutrition, longevity and disease: From molecular mechanisms to interventions. *Cell* **185**, 1455–1470 (2022).
7. C. M. McCay, F. C. Bing, W. E. Dilley, Factor H in the nutrition of trout. *Science* **67**, 249–250 (1928).
8. W. Mair, M. D. W. Piper, L. Partridge, Calories do not explain extension of life span by dietary restriction in *Drosophila*. *PLOS Biol.* **3**, e223 (2005).
9. K. P. Lee, S. J. Simpson, F. J. Clissold, R. Brooks, J. W. O. Ballard, P. W. Taylor, N. Soran, D. Raubenheimer, Lifespan and reproduction in *Drosophila*: New insights from nutritional geometry. *Proc. Natl. Acad. Sci. U.S.A.* **105**, 2498–2503 (2008).

10. S. M. Solon-Biet, A. C. McMahon, J. W. O. Ballard, K. Ruohonen, L. E. Wu, V. C. Cogger, A. Warren, X. Huang, N. Pichaud, R. G. Melvin, R. Gokarn, M. Khalil, N. Turner, G. J. Cooney, D. A. Sinclair, D. Raubenheimer, D. G. Le Couteur, S. J. Simpson, The ratio of macronutrients, not caloric intake, dictates cardiometabolic health, aging, and longevity in ad libitum-fed mice. *Cell Metab.* **19**, 418–430 (2014).
11. C. M. Hill, D. C. Albarado, L. G. Coco, R. A. Spann, M. S. Khan, E. Qualls-Creekmore, D. H. Burk, S. J. Burke, J. J. Collier, S. Yu, D. H. McDougal, H.-R. Berthoud, H. Münzberg, A. Bartke, C. D. Morrison, FGF21 is required for protein restriction to extend lifespan and improve metabolic health in male mice. *Nat. Commun.* **13**, 1897 (2022).
12. C. M. Hill, T. Laeger, M. Dehner, D. C. Albarado, B. Clarke, D. Wanders, S. J. Burke, J. J. Collier, E. Qualls-Creekmore, S. M. Solon-Biet, S. J. Simpson, H.-R. Berthoud, H. Münzberg, C. D. Morrison, FGF21 signals protein status to the brain and adaptively regulates food choice and metabolism. *Cell Rep.* **27**, 2934–2947.e3 (2019).
13. R. C. Grandison, M. D. W. Piper, L. Partridge, Amino-acid imbalance explains extension of lifespan by dietary restriction in Drosophila. *Nature* **462**, 1061–1064 (2009).
14. R. Babygirija, D. W. Lamming, The regulation of healthspan and lifespan by dietary amino acids. *Transl. Med. Aging* **5**, 17–30 (2021).
15. J. P. Richie Jr., Y. Leutzinger, S. Parthasarathy, V. Malloy, N. Orentreich, J. A. Zimmerman, Methionine restriction increases blood glutathione and longevity in F344 rats. *FASEB J.* **8**, 1302–1307 (1994).
16. B. C. Lee, A. Kaya, S. Ma, G. Kim, M. V. Gerashchenko, S. H. Yim, Z. Hu, L. G. Harshman, V. N. Gladyshev, Methionine restriction extends lifespan of *Drosophila melanogaster* under conditions of low amino-acid status. *Nat. Commun.* **5**, 3592 (2014).
17. H. Kosakamoto, F. Obata, J. Kuraishi, H. Aikawa, R. Okada, J. N. Johnstone, T. Onuma, M. D. W. Piper, M. Miura, Early-adult methionine restriction reduces methionine sulfoxide and extends lifespan in *Drosophila*. *Nat. Commun.* **14**, 7832 (2023).
18. R. A. Miller, G. Buehner, Y. Chang, J. M. Harper, R. Sigler, M. Smith-Wheelock, Methionine-deficient diet extends mouse lifespan, slows immune and lens aging, alters glucose, T4, IGF-I and insulin levels, and increases hepatocyte MIF levels and stress resistance. *Aging Cell* **4**, 119–125 (2005).
19. R. Castro-Portuguez, G. L. Sutphin, Kynurenine pathway, NAD^+ synthesis, and mitochondrial function: Targeting tryptophan metabolism to promote longevity and healthspan. *Exp. Gerontol.* **132**, 110841 (2020).
20. M. L. De Marte, H. E. Enesco, Influence of low tryptophan diet on survival and organ growth in mice. *Mech. Ageing Dev.* **36**, 161–171 (1986).
21. N. E. Richardson, E. N. Konon, H. S. Schuster, A. T. Mitchell, C. Boyle, A. C. Rodgers, M. Finke, L. R. Haider, D. Yu, V. Flores, H. H. Pak, S. Ahmad, S. Ahmed, A. Radcliff, J. Wu, E. M. Williams, L. Abdi, D. S. Sherman, T. Hacker, D. W. Lamming, Lifelong restriction of dietary branched-chain amino acids has sex-specific benefits for frailty and lifespan in mice. *Nat. Aging* **1**, 73–86 (2021).
22. C. L. Green, M. E. Trautman, K. Chaiyakul, R. Jain, Y. H. Alam, R. Babygirija, H. H. Pak, M. M. Sonsalla, M. F. Calubag, C.-Y. Yeh, A. Bleicher, G. Novak, T. T. Liu, S. Newman, W. A. Ricke, K. A. Matkowskyj, I. M. Ong, C. Jang, J. Simcox, D. W. Lamming, Dietary restriction of isoleucine increases healthspan and lifespan of genetically heterogeneous mice. *Cell Metab.* **35**, 1976–1995.e6 (2023).
23. C. Ruckenstuhl, C. Netzberger, I. Entfellner, D. Carmona-Gutierrez, T. Kickenweiz, S. Stekovic, C. Gleixner, C. Schmid, L. Klug, A. G. Sorgo, T. Eisenberg, S. Büttner, G. Mariño, R. Koziel, P. Jansen-Dürr, K.-U. Fröhlich, G. Kroemer, F. Madeo, Lifespan extension by methionine restriction requires autophagy-dependent vacuolar acidification. *PLOS Genet.* **10**, e1004347 (2014).
24. J. E. Johnson, F. B. Johnson, Methionine restriction activates the retrograde response and confers both stress tolerance and lifespan extension to yeast, mouse and human cells. *PLOS ONE* **9**, e97729 (2014).
25. G. Wu, *Amino Acids: Biochemistry and Nutrition* (CRC Press, 2013).
26. H. Kosakamoto, N. Okamoto, H. Aikawa, Y. Sugiura, M. Suematsu, R. Niwa, M. Miura, F. Obata, Sensing of the non-essential amino acid tyrosine governs the response to protein restriction in *Drosophila*. *Nat. Metab.* **4**, 944–959 (2022).
27. R. L. Wolfson, D. M. Sabatini, The dawn of the age of amino acid sensors for the mTORC1 pathway. *Cell Metab.* **26**, 301–309 (2017).
28. J. Dong, H. Qiu, M. Garcia-Barrio, J. Anderson, A. G. Hinnebusch, Uncharged tRNA activates GCN2 by displacing the protein kinase moiety from a bipartite tRNA-binding domain. *Mol. Cell* **6**, 269–279 (2000).
29. M. S. Kilberg, J. Shan, N. Su, ATF4-dependent transcription mediates signaling of amino acid limitation. *Trends Endocrinol. Metab.* **20**, 436–443 (2009).
30. B. D. Manning, A. Toker, AKT/PKB signaling: Navigating the network. *Cell* **169**, 381–405 (2017).
31. X. Gu, P. Jouandin, P. V. Lalgudi, R. Binari, M. L. Valenstein, M. A. Reid, A. E. Allen, N. Kamitaki, J. W. Locasale, N. Perrimon, D. M. Sabatini, Sestrin mediates detection of and adaptation to low-leucine diets in *Drosophila*. *Nature* **608**, 209–216 (2022).
32. T. E. Dever, L. Feng, R. C. Wek, A. M. Cigan, T. F. Donahue, A. G. Hinnebusch, Phosphorylation of initiation factor 2 alpha by protein kinase GCN2 mediates gene-specific translational control of GCN4 in yeast. *Cell* **68**, 585–596 (1992).
33. H. P. Harding, A. Ordonez, F. Allen, L. Parts, A. J. Inglis, R. L. Williams, D. Ron, The ribosomal P-stalk couples amino acid starvation to GCN2 activation in mammalian cells. *eLife* **8**, e50149 (2019).
34. A. J. Inglis, G. R. Masson, S. Shao, O. Perisic, S. H. McLaughlin, R. S. Hegde, R. L. Williams, Activation of GCN2 by the ribosomal P-stalk. *Proc. Natl. Acad. Sci. U.S.A.* **116**, 4946–4954 (2019).
35. M. E. Giannakou, L. Partridge, Role of insulin-like signalling in *Drosophila* lifespan. *Trends Biochem. Sci.* **32**, 180–188 (2007).
36. S. C. Johnson, P. S. Rabinovitch, M. Kaeberlein, mTOR is a key modulator of ageing and age-related disease. *Nature* **493**, 338–345 (2013).
37. J. B. Mannick, D. W. Lamming, Targeting the biology of aging with mTOR inhibitors. *Nat. Aging* **3**, 642–660 (2023).
38. G. Y. Liu, D. M. Sabatini, mTOR at the nexus of nutrition, growth, ageing and disease. *Nat. Rev. Mol. Cell Biol.* **21**, 183–203 (2020).
39. J. Gallinetti, E. Harputlugil, J. R. Mitchell, Amino acid sensing in dietary-restriction-mediated longevity: Roles of signal-transducing kinases GCN2 and TOR. *Biochem. J.* **449**, 1–10 (2013).
40. J. Lu, U. Temp, A. Müller-Hartmann, J. Esser, S. Grönke, L. Partridge, Sestrin is a key regulator of stem cell function and lifespan in response to dietary amino acids. *Nat. Aging* **1**, 60–72 (2021).
41. C. Géminard, E. J. Rulifson, P. Léopold, Remote control of insulin secretion by fat cells in *Drosophila*. *Cell Metab.* **10**, 199–207 (2009).
42. G. Manière, G. Alves, M. Berthelot-Grosjean, Y. Grosjean, Growth regulation by amino acid transporters in *Drosophila* larvae. *Cell. Mol. Life Sci.* **77**, 4289–4297 (2020).
43. T. Laeger, D. C. Albarado, S. J. Burke, L. Trosclair, J. W. Hedgepeth, H. R. Berthoud, T. W. Gettys, J. J. Collier, H. Münzberg, C. D. Morrison, Metabolic responses to dietary protein restriction require an increase in FGF21 that is delayed by the absence of GCN2. *Cell Rep.* **16**, 707–716 (2016).
44. B. Kim, M. I. Kanai, Y. Oh, M. Kyung, E.-K. Kim, I.-H. Jang, J.-H. Lee, S.-G. Kim, G. S. B. Suh, W.-J. Lee, Response of the microbiome-gut-brain axis in *Drosophila* to amino acid deficit. *Nature* **593**, 570–574 (2021).
45. J. Sun, C. Liu, X. Bai, X. Li, J. Li, Z. Zhang, Y. Zhang, J. Guo, Y. Li, *Drosophila* FIT is a protein-specific satiety hormone essential for feeding control. *Nat. Commun.* **8**, 14161 (2017).
46. A. P. Francisco, I. Tastekin, A. B. Fernandes, G. Ezra-Nevo, B. Deplancke, A. J. Oliveira-Maia, A. M. Gontijo, C. Ribeiro, marmite defines a novel conserved neuropeptide family mediating nutritional homeostasis. bioRxiv, 2022.12.12.520095 (2022).
47. J. Gao, S. Zhang, P. Deng, Z. Wu, B. Lemaitre, Z. Zhai, Z. Guo, Dietary L-Glu sensing by enteroendocrine cells adjusts food intake via modulating gut PYY/NPF secretion. *Nat. Commun.* **15**, 3514 (2024).
48. B. Zanco, C. K. Mirth, C. M. Sgrò, M. D. W. Piper, A dietary sterol trade-off determines lifespan responses to dietary restriction in *Drosophila melanogaster* females. *eLife* **10**, e6233 (2021).
49. A. Srivastava, J. Lu, D. S. Gadalla, O. Hendrich, S. Grönke, L. Partridge, The role of GCN2 kinase in mediating the effects of amino acids on longevity and feeding behaviour in Drosophila. *Front. Aging* **3**, 944466 (2022).
50. R. Leitão-Gonçalves, Z. Carvalho-Santos, A. P. Francisco, G. T. Fioreze, M. Anjos, C. Baltazar, A. P. Elias, P. M. Itskov, M. D. W. Piper, C. Ribeiro, Commensal bacteria and essential amino acids control food choice behavior and reproduction. *PLOS Biol.* **15**, e2000862 (2017).
51. S. A. Deshpande, E. W. Rohrbach, J. D. Asuncion, J. Harrigan, A. Eamani, E. H. Schlingmann, D. J. Suto, P.-T. Lee, F. E. Schweizer, H. J. Bellen, D. E. Krantz, Regulation of *Drosophila* oviduct muscle contractility by octopamine. *iScience* **25**, 104697 (2022).
52. M. J. Kang, D. Vasudevan, K. Kang, K. Kim, J. E. Park, N. Zhang, X. Zeng, T. A. Neubert, M. T. Marr, H. D. Ryoo, 4E-BP is a target of the GCN2-ATF4 pathway during *Drosophila* development and aging. *J. Cell Biol.* **216**, 115–129 (2017).
53. H. Kosakamoto, M. Miura, F. Obata, Epidermal tyrosine catabolism is crucial for metabolic homeostasis and survival against high-protein diets in *Drosophila*. *Development* **151**, dev202372 (2024).
54. P. Zhang, J. H. Catterson, S. Grönke, L. Partridge, Inhibition of S6K lowers age-related inflammation and increases lifespan through the endolysosomal system. *Nat. Aging* **4**, 491–509 (2024).
55. Y. Hou, Y. Yin, G. Wu, Dietary essentiality of "'nutritionally non-essential amino acids'" for animals and humans. *Exp. Biol. Med.* **240**, 997–1007 (2015).
56. C. Romano, G. Corsetti, V. Flati, E. Pasini, A. Picca, R. Calvani, E. Marzetti, F. S. Dioguardi, Influence of diets with varying essential/nonessential amino acid ratios on mouse lifespan. *Nutrients* **11**, 1367 (2019).
57. P. Viskaitis, M. Arnold, C. Garau, L. T. Jensen, L. Fugger, D. Peleg-Raibstein, D. Burdakov, Ingested non-essential amino acids recruit brain orexin cells to suppress eating in mice. *Curr. Biol.* **32**, 1812–1821.e4 (2022).
58. M. M. Karnani, J. Apergis-Schoute, A. Adamantidis, L. T. Jensen, L. de Lecea, L. Fugger, D. Burdakov, Activation of central orexin/hypocretin neurons by dietary amino acids. *Neuron* **72**, 616–629 (2011).

59. H. Hara, N. Akatsuka, Y. Aoyama, Non-essential amino acids play an important role in adaptation of the rat exocrine pancreas to high nitrogen feeding. *J. Nutr. Biochem.* **12**, 450–457 (2001).
60. J. P. Dudzic, S. Kondo, R. Ueda, C. M. Bergman, B. Lemaitre, *Drosophila* innate immunity: Regional and functional specialization of prophenoloxidases. *BMC Biol.* **13**, 81 (2015).
61. C. Scherfer, V. C. Han, Y. Wang, A. E. Anderson, M. J. Galko, Autophagy drives epidermal deterioration in a *Drosophila* model of tissue aging. *Aging* **5**, 276–287 (2013).
62. A. A. Parkhitko, D. Ramesh, L. Wang, D. Leshchiner, E. Filine, R. Binari, A. L. Olsen, J. M. Asara, V. Cracan, J. D. Rabinowitz, A. Brockmann, N. Perrimon, Downregulation of the tyrosine degradation pathway extends *Drosophila* lifespan. *eLife* **9**, e58053 (2020).
63. M. Adnan, S. Puranik, *Hypertyrosinemia* (StatPearls Publishing, 2022).
64. R. Najafi, N. Mostofizadeh, M. Hashemipour, A case of tyrosinemia type III with status epilepticus and mental retardation. *Adv. Biomed. Res.* **7**, 7 (2018).
65. Y. Xie, X. Lv, D. Ni, J. Liu, Y. Hu, Y. Liu, Y. Liu, R. Liu, H. Zhao, Z. Lu, Q. Zhou, HPD degradation regulated by the TTC36-STK33-PELI1 signaling axis induces tyrosinemia and neurological damage. *Nat. Commun.* **10**, 4266 (2019).
66. C. B. Newgard, J. An, J. R. Bain, M. J. Muehlbauer, R. D. Stevens, L. F. Lien, A. M. Haqq, S. H. Shah, M. Arlotto, C. A. Slentz, J. Rochon, D. Gallup, O. Ilkayeva, B. R. Wenner, W. S. Yancy Jr., H. Eisenson, G. Musante, R. S. Surwit, D. S. Millington, M. D. Butler, L. P. Svetkey, A branched-chain amino acid-related metabolic signature that differentiates obese and lean humans and contributes to insulin resistance. *Cell Metab.* **9**, 311–326 (2009).
67. A. Stancáková, M. Civelek, N. K. Saleem, P. Soininen, A. J. Kangas, H. Cederberg, J. Paananen, J. Pihlajamäki, L. L. Bonnycastle, M. A. Morken, M. Boehnke, P. Pajukanta, A. J. Lusis, F. S. Collins, J. Kuusisto, M. Ala-Korpela, M. Laakso, Hyperglycemia and a common variant of GCKR are associated with the levels of eight amino acids in 9,369 Finnish men. *Diabetes* **61**, 1895–1902 (2012).
68. T. J. Wang, M. G. Larson, R. S. Vasan, S. Cheng, E. P. Rhee, E. McCabe, G. D. Lewis, C. S. Fox, P. F. Jacques, C. Fernandez, C. J. O'Donnell, S. A. Carr, V. K. Mootha, J. C. Florez, A. Souza, O. Melander, C. B. Clish, R. E. Gerszten, Metabolite profiles and the risk of developing diabetes. *Nat. Med.* **17**, 448–453 (2011).
69. P. Würtz, V.-P. Mäkinen, P. Soininen, A. J. Kangas, T. Tukiainen, J. Kettunen, M. J. Savolainen, T. Tammelin, J. S. Viikari, T. Rönnemaa, M. Kähönen, T. Lehtimäki, S. Ripatti, O. T. Raitakari, M.-R. Järvelin, M. Ala-Korpela, Metabolic signatures of insulin resistance in 7,098 young adults. *Diabetes* **61**, 1372–1380 (2012).
70. S. M. Solon-Biet, V. C. Cogger, T. Pulpitel, D. Wahl, X. Clark, E. Bagley, G. C. Gregoriou, A. M. Senior, Q.-P. Wang, A. E. Brandon, R. Perks, J. O'Sullivan, Y. C. Koay, K. Bell-Anderson, M. Kebede, B. Yau, C. Atkinson, G. Svineng, T. Dodgson, J. A. Wali, M. D. W. Piper, P. Juricic, L. Partridge, A. J. Rose, D. Raubenheimer, G. J. Cooney, D. G. Le Couteur, S. J. Simpson, Branched chain amino acids impact health and lifespan indirectly via amino acid balance and appetite control. *Nat. Metab.* **1**, 532–545 (2019).
71. G. D'Antona, M. Ragni, A. Cardile, L. Tedesco, M. Dossena, F. Bruttini, F. Caliaro, G. Corsetti, R. Bottinelli, M. O. Carruba, A. Valerio, E. Nisoli, Branched-chain amino acid supplementation promotes survival and supports cardiac and skeletal muscle mitochondrial biogenesis in middle-aged mice. *Cell Metab.* **12**, 362–372 (2010).
72. J. P. Aris, A. L. Alvers, R. A. Ferraiuolo, L. K. Fishwick, A. Hanvivatpong, D. Hu, C. Kirlew, M. T. Leonard, K. J. Losin, M. Marraffini, A. Y. Seo, V. Swanberg, J. L. Westcott, M. S. Wood, C. Leeuwenburgh, W. A. Dunn Jr., Autophagy and leucine promote chronological longevity and respiration proficiency during calorie restriction in yeast. *Exp. Gerontol.* **48**, 1107–1119 (2013).
73. M. D. W. Piper, G. A. Soultoukis, E. Blanc, A. Mesaros, S. L. Herbert, P. Juricic, X. He, I. Atanassov, H. Salmonowicz, M. Yang, S. J. Simpson, C. Ribeiro, L. Partridge, Matching dietary amino acid balance to the in silico-translated exome optimizes growth and reproduction without cost to lifespan. *Cell Metab.* **25**, 610–621 (2017).
74. J. Schindelin, I. Arganda-Carreras, E. Frise, V. Kaynig, M. Longair, T. Pietzsch, S. Preibisch, C. Rueden, S. Saalfeld, B. Schmid, J.-Y. Tinevez, D. J. White, V. Hartenstein, K. Eliceiri, P. Tomancak, A. Cardona, Fiji: An open-source platform for biological-image analysis. *Nat. Methods* **9**, 676–682 (2012).
75. M. Shiota, M. Naya, T. Yamamoto, T. Hishiki, T. Tani, H. Takahashi, A. Kubo, D. Koike, M. Itoh, M. Ohmura, Y. Kabe, Y. Sugiura, N. Hiraoka, T. Morikawa, K. Takubo, K. Suina, H. Nagashima, O. Sampetrean, O. Nagano, H. Saya, S. Yamazoe, H. Watanabe, M. Suematsu, Gold-nanofève surface-enhanced Raman spectroscopy visualizes hypotaurine as a robust anti-oxidant consumed in cancer survival. *Nat. Commun.* **9**, 1561 (2018).
76. N. Toshima, T. Tanimura, Taste preference for amino acids is dependent on internal nutritional state in *Drosophila* melanogaster. *J. Exp. Biol.* **215** (Pt. 16), 2827–2832 (2012).
77. S. Andrews, FastQC: A quality control tool for high throughput sequence data (2010); www.bioinformatics.babraham.ac.uk/projects/fastqc/.
78. P. Ewels, M. Magnusson, S. Lundin, M. Käller, MultiQC: Summarize analysis results for multiple tools and samples in a single report. *Bioinformatics* **32**, 3047–3048 (2016).
79. F. Krueger, TrimGalore: A wrapper around Cutadapt and FastQC to consistently apply adapter and quality trimming to FastQ files, with extra functionality for RRBS data, Github (2015); https://github.com/FelixKrueger/TrimGalore.
80. D. Kim, J. M. Paggi, C. Park, C. Bennett, S. L. Salzberg, Graph-based genome alignment and genotyping with HISAT2 and HISAT-genotype. *Nat. Biotechnol.* **37**, 907–915 (2019).
81. M. Pertea, G. M. Pertea, C. M. Antonescu, T.-C. Chang, J. T. Mendell, S. L. Salzberg, StringTie enables improved reconstruction of a transcriptome from RNA-seq reads. *Nat. Biotechnol.* **33**, 290–295 (2015).
82. M. D. Robinson, D. J. McCarthy, G. K. Smyth, edgeR: A Bioconductor package for differential expression analysis of digital gene expression data. *Bioinformatics* **26**, 139–140 (2010).

Acknowledgments: We thank Kyoto Stock Center, National Institute of Genetics, Vienna Drosophila Resource Center, and Bloomington Drosophila Stock Center for reagents. We thank all members of our laboratory for technical assistance and critical advice. **Funding:** This work was supported by AMED-PRIME 20gm6310011 (to F.O.), Japan Society for the Promotion of Science 22K20731 (to H.K.), Japan Society for the Promotion of Science 19H03367 (to F.O.), Japan Society for the Promotion of Science 22H02769 (to F.O.), Japan Society for the Promotion of Science 21K19206 (to M.M.), Japan Society for the Promotion of Science 23H04766 (to M.M.), Japan Society for the Promotion of Science 24H00567 (to M.M.), Uehara Memorial Foundation (to F.O.), and Japan Science and Technology Agency JPMJAX2226 (to H.K.). **Author contributions:** Conceptualization: H.K. and F.O. Methodology: C.S., H.K., and F.O. Investigation: H.K. and R.O. Visualization: H.K. Supervision: F.O. and M.M. Writing—original draft: H.K. and F.O. Writing—review and editing: F.O., M.M., and C.S. **Competing interests:** The authors declare that they have no competing interests. **Data and materials availability:** All data needed to evaluate the conclusions in the paper are present in the paper and/or the Supplementary Materials. The mass spectrometry raw data generated in this study have been deposited in the DNA Data Bank of Japan (DDBJ) MetaboBank under accession codes MTBKS238, MTBKS239, MTBKS240, and MTBKS241 (https://ddbj.nig.ac.jp/public/metabobank/study/). The mass spectrometry data generated in this study are provided in data S2. RNA sequencing data have been deposited at the DDBJ under accession number PRJDB17577. All the materials generated in this study are available upon request to F.O.

Submitted 11 March 2024
Accepted 26 July 2024
Published 30 August 2024
10.1126/sciadv.adn7167